



OPTIMAL OPERATION OF ETHYLENE POLYMERIZATION REACTORS FOR TAILORED MWD

Mariano Asteasuain Adriana Brandolin¹

*Planta Piloto de Ingeniería Química (Universidad
Nacional del Sur - CONICET), Camino La Carrindanga
km 7, C.C. 717, (8000) Bahía Blanca, Argentina*

Abstract: A comprehensive steady-state model of the high-pressure ethylene polymerization in a tubular reactor that is able to calculate the complete molecular weight distribution (MWD) as function of the reactor axial distance is presented. MWD is calculated by means of the probability generating function technique. The model is implemented in gPROMS and included in an optimization framework that is used to determine optimal operating conditions for producing a polymer with tailored MWD. Two application examples are presented, the first involves maximization of conversion while maintaining the original MWD, and the second consists in finding the operating conditions needed to produce a polymer with a bimodal MWD. *Copyright © 2002 IFAC*

Keywords: Polyethylene, Polymerization, Molecular weight distribution, Mathematical models, Optimization, Tubular reactor

1. INTRODUCTION

Polyethylene is a commodity polymer with one of the most important markets among the commercial polymers, with a world annual production of about 35 million tons (Kim and Iedema, 2004). Low density polyethylene (LDPE), one of the members of the polyethylene family, is produced by high-pressure free-radical polymerization in tubular or autoclave reactors. This work focuses on the polymerization in tubular reactors to produce low density polyethylene. This is a widely used industrial process, which is carried out under rigorous operating conditions. For instance, axial velocities are usually around 11 m/s, pressures range from 1800 to 2800 bar, and temperatures are between 50°C at the reactor entrance and 335°C at the peaks. A typical reactor has a main feed consisting of ethylene monomer, a mixture

of modifiers, inerts, and oxygen initiator. In addition, there are lateral injections of peroxide initiator mixtures, which may be accompanied by monomer and/or modifiers. The reactor is divided in heating/cooling jacket zones in order to reach an appropriate reaction temperature or to control the exothermic reaction. Pressure pulsing of the reactor is sometimes applied to control polymer build-up at the reactor walls.

Driven by commercial reasons, several studies have been performed on the optimization of LDPE tubular reactors, most of which used simplified models. For instance, Mavridis and Kiparissides (1985) presented an optimization strategy using a theoretical model to find the best values of the operative parameters, so as to obtain the maximum conversion for a polyethylene of certain molecular weight. Yoon and Rhee (1985) determined optimal temperature profiles that maximized conversion. They used a simplified model without includ-

¹ Author to whom correspondence should be addressed

ing molecular properties requirements. Kiparisides *et al.* (1994) carried out an on-line optimization of a LDPE tubular reactor taking into account requirements on the polymer melt index and density. In a series of papers (Brandolin *et al.*, 1991; Asteasuain *et al.*, 2001a), a rigorous model of the reactor was used to determine optimal operating policies and reactor design features for an industrial reactor, while keeping average molecular properties within desired values.

A very important molecular property to which less attention has been paid is the complete molecular weight distribution (MWD). Optimization of the reactor operation while tailoring the MWD is a very useful application of a mathematical model, because a number of processing and end-use properties of the polymer are strongly dependent on the breadth and shape of the MWD. For example, high molecular weight tails and *shoulders* can increase the sensitivity of melt viscosity to shear rate (Wells and Ray, 2005). Several methods have been proposed to predict the complete MWD in different systems. However, applications for tailoring the MWD are not frequent. In the case of the high-pressure ethylene polymerization in tubular reactors, there are few works dealing with the calculation of the complete MWD (Wells and Ray, 2005; Schmidt *et al.*, 2005; Kim and Iedema, 2004), but none of them attempted to tailor this property in an optimization framework.

This work presents a comprehensive steady-state model of the high-pressure ethylene polymerization in a tubular reactor that is able to calculate the complete MWD as function of the reactor axial distance, and its application in optimizing the reactor operation while producing a polymer with tailored MWD. A previous model (Brandolin *et al.*, 1996) is extended to calculate the complete MWD by means of the probability generating function (pgf) technique developed by the authors (Asteasuain *et al.*, 2002a; Asteasuain *et al.*, 2002b). This technique allows modelling the MWD easily and efficiently, in spite of the reactor model complexity. Detailed modelling capabilities of the previous model are kept. The rigorous model of the polymerization reactor presented here is implemented in gPROMS (Process Systems Enterprise, Ltd.), and included in an optimization framework that is used to determine optimal operating conditions for producing a polymer with specific MWD. To the best of our knowledge, this is the first work dealing with the optimization of this process in which a tailored shape for the MWD is included. Two application examples are presented, the first involves maximization of conversion while maintaining the original MWD, and the second consists in finding the operating conditions needed to produce a polymer with a bimodal MWD.

2. MODEL DESCRIPTION

The reactor configuration is displayed in figure 1. It corresponds to a typical industrial reactor, with 8 jacket zones and 2 lateral feedings. Some of the design features are shown in the figure. The mathematical model of the polymerization reactor is based on a previous model by the authors (Brandolin *et al.*, 1996), which was extended to calculate the complete MWD. It assumes plug flow and supercritical reaction mixture; besides, it considers variation of physical and transport properties along the axial distance, calculated with rigorous correlations. Detailed calculation of the heat-transfer coefficient along the axial distance is also included (Lacunza *et al.*, 1998).

Polymer properties of interest in this work are the complete MWD and the average molecular weights. Therefore, only the reactions of the former kinetic mechanism (Brandolin *et al.*, 1996) that are crucial for the prediction of the mentioned properties, as well as the conversion and temperature profiles, were kept. The kinetic mechanism is shown in table 1.

Table 1. Kinetic mechanism.

<i>Peroxide Initiation</i>	
I_k	$\xrightarrow{k_{ik}} 2R(0) \quad k = 1, 2$
<i>Oxygen Initiation</i>	
$O_2 + M$	$\xrightarrow{k_o} 2R(0)$
<i>Monomer thermal initiation</i>	
$3M$	$\xrightarrow{k_{mi}} R(1) + R(2)$
<i>Generation of inert</i>	
$O_2 + R(m)$	$\xrightarrow{f_o k_o} X$
<i>Propagation</i>	
$R(m) + M$	$\xrightarrow{k_p} R(m+1)$
<i>Termination by combination</i>	
$R(n) + R(m)$	$\xrightarrow{k_{tc}} R(n+m)$
<i>Thermal degradation</i>	
$R(m)$	$\xrightarrow{k_{td}} P(m) + R(0)$
<i>Chain transfer to monomer</i>	
$R(m) + M$	$\xrightarrow{k_{trm}} P(m) + R(1)$
<i>Chain transfer to polymer</i>	
$R(n) + P(m)$	$\xrightarrow{m k_{trp}} P(n) + R(m)$
<i>Chain transfer to modifier</i>	
$R(m) + S$	$\xrightarrow{k_{trs}} P(m) + R(0)$

Symbols M , I , O_2 and S stand for ethylene monomer, peroxide initiator, oxygen and modifier, respectively; $P(m)$ and $R(m)$ are polymer and living radical molecules, respectively, of chain length m .

In order to avoid iterative calculations that increase the computational burden, the jacket temperature at each one of the eight reaction zones was assumed constant, and the pressure pulse was neglected. Besides, peroxide and modifier mixtures are treated as single fictitious species. These simplifications were validated in a subsequent work by the authors (Asteasuain *et al.*, 2001b),

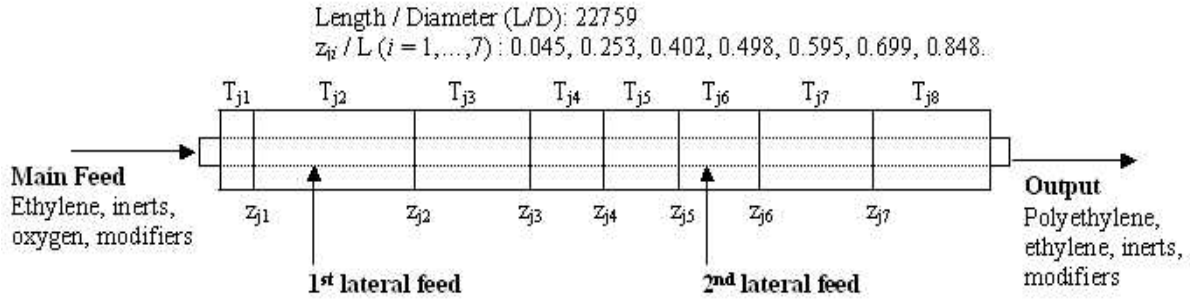


Fig. 1. Tubular reactor for high-pressure ethylene polymerization

against several data sets from an industrial tubular reactor. The set of kinetic constants obtained in Astasuain *et al.* (2001b) are used here.

The set of the main model equations is listed in table 2. In these equations, ρ and C_p are the density and heat-capacity of the reaction mixture, v is the axial velocity, T and T_j are the reactor and jacket temperatures, and P is the reactor pressure; U , D , ΔH , f_f and Mw_j are the global heat-transfer coefficient, reactor internal diameter, propagation reaction enthalpy, friction factor and molecular weight of the j component; λ_a and μ_a are the a th order moments of the radical and polymer chain length distribution; r_j and r_Ψ are the generation rate of the j and Ψ entities, respectively; r_{pm} is the reaction rate of the propagation reaction; F_{main} is the global mass flow at the reactor entrance; \bar{F}_j is the molar flow per unit length of the j component; $\phi_{a,l}$ and $\varphi_{a,l}$ are the probability generating functions (pgf) of the radical and polymer chain length distribution ($a = 0, 1, 2$ is related to the MWD expressed in number, weight and chromatographic (mass times the molecular weight) fraction, respectively, as shown in table 2, and l is the dummy variable of the pgf); $n(m)$, $w(m)$ and $c(m)$ are the number, weight and chromatographic fraction of the macromolecule of chain length m . Expressions corresponding to the terms r_j and r_Ψ can be found elsewhere (Astasuain and Brandolin, 2005). The molar flows per unit length \bar{F}_j are used to model the lateral feedings to the reactor (Astasuain and Brandolin, 2005).

The innovation of the present model is the addition of the calculation of the complete MWD along the axial distance. The MWD is calculated, independently, in number, weight and chromatographic fraction. This is performed by means of the probability generating function (pgf) technique developed by the authors (Astasuain *et al.*, 2002a; Astasuain *et al.*, 2002b). With this technique, first the mass balances of the generic species $R(m)$ and $P(m)$ are transformed into the pgf domain, obtaining the balance equations for $\phi_{a,l}$ and $\varphi_{a,l}$. Then, from the solution of these

Table 2. Main model equations.

<i>Global mass balance</i>
$\rho(z) v(z) = F_{main} + \int_0^z \left(\sum_j \bar{F}_j(z) Mw_j \right) dz$
<i>Mass balances of components</i>
$\frac{d(C_j(z) v(z))}{dz} = -r_j(z) + \bar{F}_j(z)$
$j = O_2, M, I_k (k = 1, 2), S$
<i>Mass balances of moments and pgfs</i>
$\frac{d(\Psi(z) v(z))}{dz} = -r_\Psi(z)$
$\Psi = \lambda_a, \mu_a, \phi_{a,l}, \varphi_{a,l} (a = 0, 1, 2)$
<i>Energy balance</i>
$\rho(z) v(z) C_p(z) \frac{dT(z)}{dz} = -\frac{4U(z)(T(z)-T_j)}{D} + r_{pm}(z)(-\Delta H) + \bar{C}_p (T_{inlet} - T(z)) * \sum_j \bar{F}_j Mw_j$
<i>Pressure drop</i>
$\frac{dP(z)}{dz} = -\rho(z) \left(v(z) \frac{dv(z)}{dz} + \frac{2f_f v(z)^2}{D} \right)$
<i>Number average molecular weight</i>
$Mn(z) = Mw_M \frac{\lambda_1(z) + \mu_1(z)}{\lambda_0(z) + \mu_0(z)}$
<i>Weight average molecular weight</i>
$Mw(z) = Mw_M \frac{\lambda_2(z) + \mu_2(z)}{\lambda_1(z) + \mu_1(z)}$
<i>Monomer conversion</i>
$x(z) = \frac{\mu_1(z)}{\mu_1(z) + C_M(z)}$
<i>Polymer MWDs</i>
$n(m, z) = f(\varphi_{0,l}(z)), w(m, z) = f(\varphi_{1,l}(z))$
$c(m, z) = f(\varphi_{2,l}(z))$

equations and an appropriate numerical inversion of the pgfs, the complete MWDs are obtained. The inversion step is represented by function $f(\varphi_{a,l}(z))$ in table 2. The inversion of the pgfs is carried out using Stehfest's algorithm (Astasuain *et al.*, 2002a). The pgf technique allowed modelling the MWD easily and efficiently, in spite of the complexity of the reactor model. The resulting model also keeps the capabilities of the former model to calculate the following quantities along the axial distance: monomer conversion, reaction mixture temperature and pressure, mass fraction of oxygen, peroxides, monomer, radicals and polymer; average molecular weights; Peclet, Nusselt, Reynolds and Prandtl numbers, global heat-transfer coefficient, velocity, viscosity and specific heat. As mentioned before, the LDPE reactor model was implemented in gPROMS (Process Systems Enterprise, Ltd.)

3. OPTIMIZATION OF THE LDPE TUBULAR REACTOR

3.1 First case study

The first case study involved the optimization of the base case operating conditions in order to maximize conversion, while keeping the production of a polymer with the same MWD. A set of 19 optimization variables was considered, involving flow rates of different components in the main and lateral feedings, the inlet temperature and pressure and location of the lateral feedings. Optimization variables are listed in table 3. Base case operating conditions, corresponding to the production of a typical commercial polyethylene in an actual industrial reactor, are shown in the same table. Two optimization problems were solved: in the first one the lateral feedings should be at the same temperature of the main feed stream (*cold* lateral feedings); in the second, the temperature was assumed to be equal to the reactor temperature at the injection point (*hot* lateral feedings). The maximum allowed deviation with respect to the original MWD was specified by adding the constraints shown in equations 1 and 2 to the optimization problem.

$$\sum_i \left(\frac{w_{\text{new}}(m_i, z_{\text{max}}) - w_{\text{orig}}(m_i)}{w_{\text{orig}}(m_i)} \right)^2 \leq 0.01 \quad (1)$$

$$\sum_i \left(\frac{c_{\text{new}}(m_i, z_{\text{max}}) - c_{\text{orig}}(m_i)}{c_{\text{orig}}(m_i)} \right)^2 \leq 0.01 \quad (2)$$

An upper bound was imposed on the reaction mixture temperature along the axial distance to ensure safe operating conditions (thermal runaway occurs at 345°C) (Kiparissides *et al.*, 1994):

$$T(z) \leq 335^\circ\text{C} \quad (3)$$

Besides, an upper bound was also considered for the reactor temperature at the reactor exit, required for downstream process units:

$$T(z_{\text{max}}) \leq 285^\circ\text{C} \quad (4)$$

A constraint in the total monomer feed to the reactor (main feed plus lateral feedings) was applied, so as to keep the same flow rate as in the base case:

$$A \left(F_{M,\text{main}} + \int_0^z \bar{F}_M(z) M w_M dz \right) = 11 \frac{\text{kg}}{\text{s}} \quad (5)$$

where A is the cross-sectional area of the reactor.

Lower and upper bounds for the optimization variables were selected according to the usual operating conditions of an industrial reactor. Finally, the optimization problem involved maximizing conversion at the reactor exit ($x(z_{\text{max}})$) subject to the reactor model and the constraints shown in equations 1–5. The optimization was solved using the commercial software gPROMS (Process Systems Enterprise, Ltd.).

3.2 Second case study

The second case study involved the optimization of the operating conditions in order to synthesize a polymer with a tailored MWD. A bimodal distribution was selected as the *target* distribution because it is very difficult to obtain under usual operating conditions. For instance, in a set of 31 operating cases taken from an actual industrial reactor, only polyethylene with monomodal distribution was produced. In order to show the flexibility of this approach to determine the *target* MWD, only the existence of a local minimum, a necessary condition for a bimodal distribution, and its approximate location were specified (equations 6 and 7). Chain length values m_1 , m_2 and m_3 were selected so that the corresponding molecular weights ($m_i M w_M$) were, respectively, 44380, 224000 and 280000 g/mol. The objective function of the optimization problem (equation 8) was meant to increase the height of the right shoulder of the distribution.

$$c(m_2, z_{\text{max}}) - c(m_1, z_{\text{max}}) \leq 0 \quad (6)$$

$$c(m_2, z_{\text{max}}) - c(m_3, z_{\text{max}}) \leq 0 \quad (7)$$

$$FO = \min c(m_2, z_{\text{max}}) - c(m_3, z_{\text{max}}) \quad (8)$$

Equations 6 and 7 replace equations 1 and 2 in the optimization formulation. Besides, a lower bound on the monomer conversion was added to avoid uneconomical operation:

$$x(z_{\text{max}}) \geq 0.2 \quad (9)$$

The same set of optimization variables as in the previous case was used, plus the possibility of adding a lateral injection of modifier.

4. RESULTS AND DISCUSSION

Optimization results for the first case study are shown in table 3. It can be seen that the monomer conversion has been significantly increased. The success in maintaining the original MWD can be

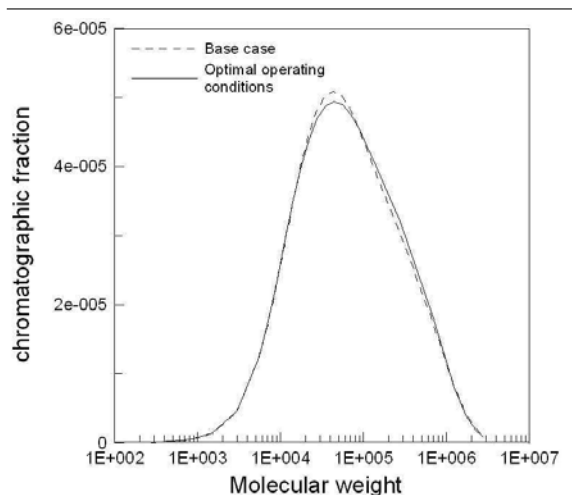


Fig. 2. Comparison of the original and final MWD. First case study

observed in figure 2, in which the original and final chromatographic MWDs are depicted. An even closer matching was obtained for the weight MWD.

Table 3. Optimal operating conditions. First case study.

Variable	Base Case	Optimal
Inlet temperature (°C)	77	72
Inlet pressure (bar)	2300	2800
Oxygen flow rate (kg/s)	$6.9 \cdot 10^{-5}$	$7.7 \cdot 10^{-5}$
Modifier flow rate (kg/s)	0.00762	0.2
Peroxide. 1 st injection (kg/s)	0.00102	$6.1 \cdot 10^{-4}$
Peroxide. 2 nd injection (kg/s)	$1.57 \cdot 10^{-4}$	$8.3 \cdot 10^{-5}$
Monomer. Main feed (kg/s)	11	11
Monomer 1 st injection (kg/s)	0	0
Monomer 2 nd injection (kg/s)	0	0
Location of 1 st injection (m)	160	49
Location of 2 nd injection (m)	840	833
Jacket temp. Zones 1-8 (°C)	170-225	153-249
	170-170	150-150
	170-170	150-150
	170-170	150-150
Conversion	25%	30%

Figure 3 shows the temperature profiles corresponding to the base case and to the optimal operating conditions. Notice that the path and end point constraints on the reactor temperature (equations 3 and 4) are satisfied.

Optimization results were the same when using *cold* or *hot* lateral feedings. This is an expected result, as the optimal point involves only initiator lateral addition, which for its small amount does not contribute significantly to the reaction mixture enthalpy. Notice that the whole monomer feed is used in the main stream, and that the first injection point has been moved nearer to the reactor entrance. Besides, a higher solvent flow rate is used to achieve the same molecular properties in spite of the conversion increase. These results are consistent with previous studies on this reactor (Asteasuain *et al.*, 2001a).

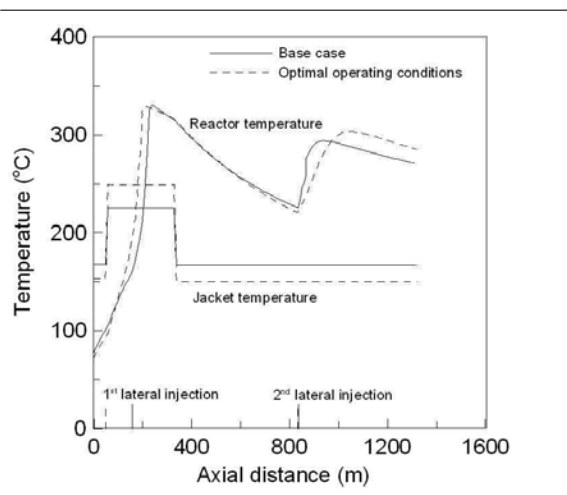


Fig. 3. Temperature profiles corresponding to the base case and to the optimal operating conditions. First case study

Figure 4 shows the resulting MWD for the second case study. A comparison of the distributions after the first reaction zone and at the reactor exit is presented. A clear bimodality at the reactor exit can be observed, showing the success of the optimization procedure. The set of the optimal operating conditions are shown in table 4.

Table 4. Optimal operating conditions. Second case study.

Variable	Base Case	Optimal
Inlet temperature (°C)	77	70
Inlet pressure (bar)	2300	2800
Oxygen flow rate (kg/s)	$6.9 \cdot 10^{-5}$	$5.9 \cdot 10^{-5}$
Modifier. Main feed (kg/s)	0.00762	0.12
Modifier. 1 st injection (kg/s)	0	$3.5 \cdot 10^{-3}$
Modifier. 2 nd injection (kg/s)	0	0.9
Peroxide. 1 st injection (kg/s)	0.00102	$2.4 \cdot 10^{-4}$
Peroxide. 2 nd injection (kg/s)	$1.57 \cdot 10^{-4}$	$8.6 \cdot 10^{-5}$
Monomer. Main feed (kg/s)	11	9.4
Monomer. 1 st injection (kg/s)	0	0.6
Monomer. 2 nd injection (kg/s)	0	1
Location of 1 st injection (m)	160	41
Location of 2 nd injection (m)	840	498
Jacket temp. Zones 1-8 (°C)	170-225	154-150
	170-170	270-226
	170-170	176-170
	170-170	270-270
Conversion	25%	25%

The operating scenario is very different to the previous ones. Notice that now the monomer feed is split between the two lateral injections, and that side injections of modifiers are also used, with an important addition in the second injection. This radical change in the process conditions was not unexpected since a polymer with a very different MWD was to be produced. Other authors (Kim and Iedema, 2004) have also found that lateral additions of modifiers are necessary to obtain bimodal MWDs in tubular reactors.

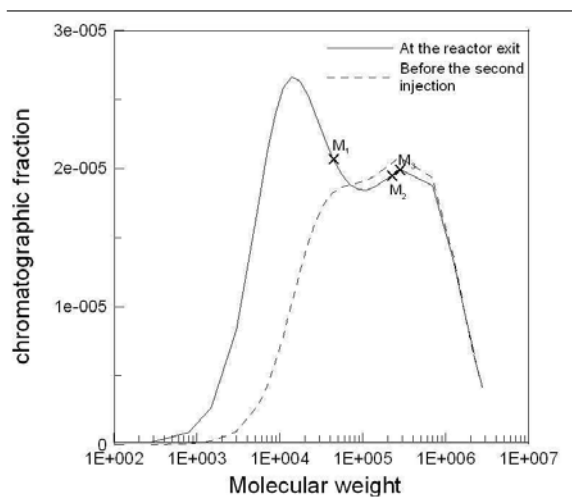


Fig. 4. Bimodal MWD. Second case study

It is interesting to see in figure 4 that the polymer formed after the first lateral injection is of high molecular weight, contributing with the right shoulder of the distribution, while the lower molecular weight polymer produced after the second injection (which involves an important addition of modifier) is responsible for the left shoulder of the distribution.

5. CONCLUSIONS

In this work we present a comprehensive steady-state model of the high-pressure ethylene polymerization in a tubular reactor that is able to calculate the complete MWD as function of the reactor axial distance, and its application in optimizing the reactor operation while producing a polymer with tailored MWD. This is performed via an optimization approach that allows great flexibility for specifying the *target* MWD and other process constraints. The two case studies presented here, the first involving maximization of conversion while maintaining the original MWD, and the second consisting in finding the operating conditions necessary to produce a polymer with a bimodal MWD, show the potential benefits of using this tool.

6. ACKNOWLEDGEMENTS

The authors wish to thank Universidad Nacional del Sur (Bahía Blanca, Argentina) and CONICET (Argentina) for financial support.

REFERENCES

Asteasuain, M., A. Brandolin and C. Sarmoria (2002a). Recovery of molecular weight distributions from transformed domains. Part II: application of numerical inversion methods. *Polymer* **43**, 2529–2541.

Asteasuain, M. and A. Brandolin (2005). Comprehensive mathematical model for a high-pressure ethylene polymerization reactor developed in gPROMS. Submitted to *Comput. Chem. Eng.*

Asteasuain, M., C. Sarmoria and A. Brandolin (2002b). Recovery of molecular weight distributions from transformed domains. Part I: application of pgf to mass balances describing reactions involving free radicals. *Polymer* **43**, 2513–2527.

Asteasuain, M., P.E. Ugrin, M.H. Lacunza and A. Brandolin (2001a). Effect of multiple feedings in the operation of a high-pressure polymerization reactor for ethylene polymerization. *Polym. React. Eng.* **9**, 163–182.

Asteasuain, M., S. Pereda, M.H. Lacunza, P.E. Ugrin and A. Brandolin (2001b). Industrial high pressure ethylene polymerization initiated by peroxide mixtures: a reduced mathematical model for parameter adjustment. *Polym. Eng. Sci.* **41**, 711–726.

Brandolin, A., E.M. Valles and J.N. Farber (1991). High pressure tubular reactor for ethylene polymerization. Optimization aspects. *Polym. Eng. Sci.* **31**, 381–390.

Brandolin, A., M.H. Lacunza, P.E. Ugrin and N.J. Capiati (1996). High pressure polymerization of ethylene. An improved mathematical model for industrial tubular reactors. *Polym. React. Eng.* **4**, 193–241.

Kim, D. and P.D. Iedema (2004). Molecular weight distribution in low-density polyethylene polymerization; Impact of scission mechanisms in the case of a tubular reactor. *Chem. Eng. Sci.* **59**, 2039–2052.

Kiparissides, C., G. Verros and A. Pertsinidis (1994). On-line optimization of a high-pressure low-density polyethylene tubular reactor. *Chem. Eng. Sci.* **49**, 5011–5024.

Lacunza, M.H., P.E. Ugrin, A. Brandolin and N.J. Capiati (1998). Heat transfer coefficient in a high pressure tubular reactor for ethylene polymerization. *Polym. Eng. Sci.* **38**, 992–1013.

Mavridis, H. and C. Kiparissides (1985). Optimization of a high-pressure polyethylene reactor. *Polym. Proc. Eng.* **3**, 263–290.

Schmidt, C., M. Busch, D. Lilge and M. Wulkow (2005). Detailed molecular structure modeling – a path forward to designing application properties of ldPE. *Macromol. Mater. Eng.* **290**, 404–414.

Wells, G.J. and W.H. Ray (2005). Prediction of polymer properties in ldpe reactors. *Macromol. Mater. Eng.* **290**, 319–346.

Yoon, B.J. and H.K. Rhee (1985). A study of the high-pressure polyethylene tubular reactor. *Chem. Eng. Commun.* **34**, 253–265.